Neuroscience Research 65 (2009) 175–186

Contents lists available at ScienceDirect

Neuroscience Research

journal homepage: www.elsevier.com/locate/neures

An investigation of cross-modal plasticity of effective connectivity in the blind by dynamic causal modeling of functional MRI data

Takeshi Fujii [a,b], Hiroki C. Tanabe [a,b], Takanori Kochiyama [c], Norihiro Sadato [a,b,d,e,*]

[a] Division of Cerebral Integration, Department of Cerebral Research, National Institute for Physiological Sciences, Okazaki, Japan
[b] Department of Physiological Sciences, The Graduate University for Advanced Studies (Sokendai), Okazaki, Japan
[c] Advanced Telecommunications Research Institute International Brain Activity Imaging Center, Seikacho, Japan
[d] Research Institute of Science and Technology for Society (RISTEX), Japan Science and Technology Agency (JST), Tokyo, Japan
[e] Biomedical Imaging Research Center, University of Fukui, Eiheiji, Japan

ARTICLE INFO

Article history:
Received 16 April 2009
Received in revised form 26 June 2009
Accepted 29 June 2009
Available online 4 July 2009

Keywords:
Blind
Braille
Dynamic causal modeling
fMRI
Plasticity
Visual cortex

ABSTRACT

To investigate connectivity between primary somatosensory area (S1) and striate cortex (V1) in the blind, we used dynamic causal modeling of functional MRI acquired while 15 blind (9 early-onset and 6 late-onset) and 24 sighted subjects performed a tactile Braille discrimination task with their right hand. Five regions of interest were selected from either the ventral or dorsal pathways: left S1, anterior intraparietal sulcus (aIPS), superior occipital gyrus (SOG), inferior occipital gyrus (IOG), and V1. Bayesian model comparison showed that a cortico-cortical feedback pathway model without direct connections between V1 and S1 performed better than that with direct connections. In the blind, baseline connectivity and its discrimination-specific modulation in aIPS–SOG and aIPS–IOG were positive and bi-directional, while they were negative in the sighted. Thus visual deprivation may induce reorganization of the visual cortical areas due to the competitive shift for tactile inputs. The early blind showed stronger connectivity than the late blind in the dorsal pathway (aIPS–V1 through SOG) and in SOG–IOG bi-directionally. Task performance positively correlated with baseline connectivity of SOG–V1 and SOG–IOG across blind subjects. Therefore, dorsal visual regions are involved in the functional shift in V1 from visual to tactile information processing in blind subjects.

1. Introduction

Braille is a well-known tactile substitution for visual letter forms used by the blind, consisting of patterns of raised dots that can be read with the fingertips. Neural substrates for Braille reading in blind people have been explored using various imaging methods. Using F-18 fluoro-deoxy-glucose (FDG)–PET, Wanet-Defalque et al. (1988) showed a high rate of glucose utilization in the occipital cortex in early-blind subjects, suggesting that visual areas are activated by tactile stimuli in the absence of visual input. Using electroencephalography (EEG), Uhl et al. (1991) found evidence to suggest that tactile inputs could produce occipital cortex activation in blind subjects. Using PET with O-15 water, the occipital cortex, including the striate cortex, was activated when early-onset blind subjects read Braille and carried out other tactile discrimination tasks (Sadato et al., 1998, 1996), a finding which was later confirmed in fMRI investigations (Amedi et al., 2003; Burton et al., 2002; Sadato et al., 2002). Together, these results suggest that visual deprivation induces plastic changes in the patterns of activation observed in occipital cortex.

In addition, it was revealed that these changes are age-dependent: tactile discrimination tasks activated the extrastriate cortex of both early-onset (<16 years old) and late-onset (>16 years old) blind subjects, whereas striate cortex was activated only in the early-onset group (Sadato et al., 2002). Moreover, these changes in neural activation appear to be related to visual deafferentation rather than long-term learning, as late-onset blind subjects who were naïve to Braille also showed activation in the extrastriate cortex during a tactile discrimination task (Sadato et al., 2004). These findings suggest that visual deprivation in early life is related to the patterns of striate cortex activation during Braille reading.

Lesion and pseudo-lesion studies have also explored the functional relevance of the occipital cortex activation by tactile input in blind participants. Cohen et al. (1997) applied repetitive transcranial magnetic stimulation (rTMS) to the mid-occipital region of blind and sighted subjects, and showed that this

* Corresponding author at: Division of Cerebral Integration, Department of Cerebral Research, National Institute for Physiological Sciences, 38 Nishigonaka, Myodaiji, Okazaki, Aichi 444-8585, Japan. Tel.: +81 564 55 7841; fax: +81 564 52 7786.
E-mail address: sadato@nips.ac.jp (N. Sadato).

0168-0102/$ – see front matter © 2009 Elsevier Ireland Ltd and the Japan Neuroscience Society. All rights reserved.
doi:10.1016/j.neures.2009.06.014

interfered with tactile perception in blind, but not sighted, participants. Cohen et al. (1999) also showed that this interference depended on the age of onset of blindness: early-onset blind subjects (<14 years old) showed increased error rates following TMS stimulation of the occipital pole, whereas no such effect was seen in late-onset blind subjects (>14 years old). In addition, Hamilton et al. (2000) report the case of an early-onset blind woman, previously a proficient Braille reader, who lost the ability to read Braille when she suffered an ischemic insult to the bilateral occipital cortices. Performance on tactile perception tasks remained unchanged (Hamilton et al., 2000). These findings indicate that occipital cortex activation in early-onset blind people may be functionally relevant to tactile information processing. Occipital cortex may in addition play a functional role in auditory processing in early-onset blind (Kujala et al., 1995; Leclerc et al., 2000; Roder et al., 1999; Weeks et al., 2000). However, the neural pathways which mediate the functional changes in the striate cortex of blind individuals remain unclear.

Bavelier and Neville (2002) have proposed three possible candidate pathways. One is a cortico-cortical feedback pathway from primary somatosensory cortex (S1) through posterior parietal cortex, which is considered to be a higher multimodal association area. Studies suggest that the anterior parts of the intraparietal sulcus (IPS), comprising the anterior intraparietal area (AIP) and ventral intraparietal area (VIP), may be regions in which visuo-tactile multimodal information of object features and motion processing is integrated in sighted subjects (Bremmer et al., 2001; Grefkes et al., 2002). In blind subjects, who lack bottom-up visual processing, tactile inputs from multimodal areas may lead to the functional recruitment of visual association cortex due to the competitive shift away from visual inputs and towards other modalities. A second, more hypothetical candidate pathway, is the direct long-range connectivity between the primary visual and somatosensory cortices (Falchier et al., 2002; Rockland and Ojima, 2003), a role for which is suggested by recent studies indicating the presence of cross-modal interactions at 'low-level' sensory cortices (Driver and Noesselt, 2008; Kayser and Logothetis, 2007; Lakatos et al., 2007; Martuzzi et al., 2007). The third candidate is a subcortical pathway, whereby the lateral geniculate nucleus is re-wired so as to transport tactile information to striate cortex (Bronchti et al., 1989). It is less likely that the subcortical pathway is relevant in humans, as previous studies have shown atrophy of the geniculo-cortical tracts in early-onset blind subjects (Noppeney et al., 2005; Shimony et al., 2006). In addition, rTMS over S1 evoked activation of peri-striate cortex without thalamic activation in early-onset but not in late-onset blind or sighted participants, suggesting that recruitment may be mediated through altered cortico-cortical pathways rather than subcortical pathways (Wittenberg et al., 2004). Thus, we did not pursue the possibility of a subcortical pathway in the present study.

There are several neuroimaging findings which support a cortico-cortical feedback pathway rather than direct long-range connectivity between the primary visual and somatosensory cortices. Preferential activation of extrastriate cortex compared to the striate cortex was observed during Braille reading (Amedi et al., 2003; Burton, 2003). Moreover, in late-onset blind subjects, extrastriate but not striate cortex was activated by a tactile discrimination task (Sadato et al., 2002). These findings suggest that striate cortex is not likely to be the cortical "entry node" for tactile signals, which would then be redirected to the visual cortices following visual deprivation. Hence, the cortico-cortical feedback pathway is the most likely of the three candidate pathways.

Assuming striate cortex receives input through a cortico-cortical feedback pathway, the candidate pathway from posterior parietal cortex to striate cortex may exist through either the dorsal or the ventral visual streams (Mishkin et al., 1983), or a combination of the two. In fact, the involvement of both dorsal and ventral visual regions in cross-modal plastic changes has been reported, implying that these regions are part of the cortico-cortical feedback pathway. Dorsal visual regions in the blind show increased activity after training on a naïve tactile task using their tongue (Ptito et al., 2005). In addition, ventral visual regions, including part of the lateral occipital complex (LOC), show multimodal shape-related activation in blind and sighted participants (Amedi et al., 2001, 2007). Thus, the main input pathway to the striate cortex remains unclear.

The purpose of the present study was to investigate the input pathway to the striate cortex of blind participants during Braille reading. We hypothesized that the main tactile input pathway to striate cortex is a cortico-cortical feedback pathway via dorsal and/or ventral streams, and that differences in the effective connectivity of these regions will differ between early-blind, late-blind and sighted groups. To evaluate the effective connectivity – the influence that one neural system exerts over another (Friston, 1994) – we used dynamic causal modeling (DCM), which provides a mechanistic model of the causal effects that optimally predict the imaging data (Friston et al., 2003). Specifically, we tested whether the dorsal or ventral visual pathways are involved while blind subjects complete tactile tasks. Data from previous functional magnetic resonance imaging (fMRI) studies (Harada et al., 2004; Sadato et al., 2002) were reanalyzed using DCM analysis. In both these studies, blind and sighted subjects performed a Braille tactile discrimination task and Braille tactile non-discrimination task.

2. Materials and methods

We reanalyzed data sets from Sadato et al. (2002) and Harada et al. (2004). Subjects, stimuli, tasks, and fMRI data acquisition are described in detail in these previous investigations. Here, we describe them briefly.

2.1. Subjects

Fifteen blind subjects, 4 female and 11 male, aged 43.9 ± 12.3 years (mean ± SD), participated in the study. Nine participants who had lost their sight before the age of 16 years were included in the early-blind group (43.6 ± 13.5 years old), and the others, who became blind after the age 16 years, were defined as the late-blind group (44.5 ± 11.5 years old). This distinction was made on the basis of a previous investigation which showed that the first 16 years of life are critical for the functional shift in V1 from processing visual to processing tactile stimuli (Sadato et al., 2002). All blind subjects were blind due to dysfunction at the level of the eye or early in the optic nerve. Control subjects were 24 sighted volunteers, 11 female and 13 male, aged 25.7 ± 4.1 years. The subjects were all right-handed according to the Edinburgh handedness inventory (Oldfield, 1971). There was no history of neurological or psychiatric illness in any of the subjects, and except for the blindness, none had any neurological deficits. The protocol was approved by the ethical committee of Fukui Medical University, and all subjects gave their written informed consent to participate.

2.2. Stimuli and tasks

The experimental procedure consisted of two tasks, a Braille tactile discrimination task (DT) and Braille tactile non-discrimination task (NDT), both of which were interleaved with rest conditions. In the DT, pairs of two-dot Braille characters were presented serially. The characters were presented passively to the subject's right index finger such that active exploration was not necessary. The subject had to respond whether the characters were the same or not by pushing a button with their left index finger or middle finger. In the NDT, a sensorimotor control task, six-dot Braille characters were presented, and the subject had to alternately push a button with their left index or middle finger irrespective of the Braille character presented. In the rest condition of each task, tactile stimuli were not given, and the subject responded by making alternate cued (see below) button presses as in the NDT.

The DT and NDT were administered in separate sessions. Each procedure consisted of 12 blocks of 30 s each, in which 6 experimental blocks of DT or NDT blocks alternated with 6 rest blocks. Each experimental block of DT or NDT consisted of 5 trials. In each trial of the experimental blocks, a pair of Braille characters was presented for 3 s and subject was required to respond in the proceeding 3 s. For blind subjects, the pacemaking response cue was a touch to the subject's left toe given every 6 s by the examiner, while for sighted subjects the cue was projected onto a semitransparent screen. The pacemaking cues were given not

only during the task period but also during the rest period in both the DT and NDT sessions for both the blind and sighted groups. Thus, the task-related activation should not be affected by the response cuing.

2.3. Functional magnetic resonance imaging data acquisition

Images were acquired using a 3 Tesla scanner (Signa Horizon; General Electric, Milwaukee, WI) using echo planar imaging. The scanning parameters were: repetition time (TR), 3000 ms; echo time (TE), 30 ms; flip angle, 90°; matrix size, 64 × 64; field of view, 22 cm; slice thickness, 3.5 mm; gap, 0.5 mm; number of slices, 36. These parameters resulted in a voxel size of 3.44 mm × 3.44 mm × 3.5 mm. Two sessions of 6 min 18 s (126 images) were acquired. A high-resolution, T2-weighted three-dimensional image was also acquired for each subject (fast-spin echo images in a steady state; matrix size, 256 × 256; pixel size, 0.859 mm × 0.859 mm; slice thickness, 1.5 mm; number of slices, 112).

2.4. Image data analysis

The results previously reported by Sadato et al. (2002) and Harada et al. (2004) were obtained using SPM99. To enable the use of DCM, we reanalyzed the data using SPM5 revision 748 (Wellcome Department of Imaging Neuroscience, London, UK, http://www.fil.ion.ucl.ac.uk/spm). For each subject, after discarding the first 6 images of each session, the remaining 240 images were realigned to correct for head motion, spatially normalized to the EPI template brain of the Montréal Neurological Institute (MNI), and resampled, resulting in 2 mm × 2 mm × 2 mm voxels, and smoothed spatially with an isotropic Gaussian kernel of 8 mm full-width half-maximum (FWHM).

Statistical analysis was conducted at two levels. First, individual task-related activation was evaluated. Second, to make inferences at a population level, individual data were summarized into a random effects model (Holmes and Friston, 1998).

Data from both DT and NDT sessions were modeled with a single subject-specific general linear convolution model to allow the effects of discrimination as a modulatory or bi-linear effect to be modeled in subsequent DCM analyses. It was modeled with two conditions of interest (tactile stimulation and tactile discrimination) and effects of no interest (session effects and realignment parameters to account for motion-related variance). The data were high-pass filtered with a cut-off period of 120 s to remove low-frequency signal drifts. A first-order autoregressive model was used to remove serial correlations in the data. Contrast images were created for each subject and for each condition (tactile stimulation and tactile discrimination).

Contrast images of tactile stimuli and discrimination conditions were used for the group analysis (Holmes and Friston, 1998). The contrast images obtained by the individual analyses represent the normalized task-related changes of the MR signal for each subject. We constructed a random effects model with a 2 (group; blind vs. sighted) × 2 (condition; tactile stimuli vs. discrimination) factorial design.

2.5. Regions of interest selection and time series extraction

To address anatomical variability and allow for more accurate estimation of interregional coupling, the regions of interest (ROIs) were determined on an individual basis, an approach utilized in previous DCM investigations (Bitan et al., 2005; Grol et al., 2007; Kumar et al., 2007; Stephan et al., 2007a). In cases where subject-specific local maxima within twice the FWHM of the smoothing kernel were not identified, group coordinates were applied in subsequent analyses.

All regions of interest used in the DCM analysis met two requirements, one of which was a functional constraint and the second was an anatomical constraint. First, to depict the regions which showed any condition-specific deviation from the overall mean, *F*-contrasts of the conditions were made in both blind and sighted groups. Then, a conjunction analysis of the *F*-contrasts of the blind and sighted groups was conducted with a conjunction null hypothesis (Friston et al., 2005). The design matrix and contrast matrix of the conjunction analysis in SPM is shown in Fig. 1a. The statistical threshold was set at a false discovery rate (FDR) of $p < 0.05$ (Genovese et al., 2002). The FDR is the proportion of false positives (incorrect rejections of the null hypothesis) among multiple voxel-wise tests for which the null hypothesis is rejected. In this way, we depicted the regions which were perturbed positively or negatively by tactile stimuli or discrimination in both blind and sighted groups.

Within these functionally constrained voxels, we added the anatomical constraints of each ROI. We selected five regions within the left hemisphere contralateral to the hand used for task performance: primary somatosensory cortex (S1); anterior intraparietal sulcus (aIPS), a multimodal area in the posterior parietal cortex; superior occipital gyrus (SOG) in the dorsal visual stream; inferior occipital gyrus (IOG) in the ventral visual stream; and striate cortex (primary visual cortex, V1) (Fig. 1b). To simplify the model, only left hemisphere regions were included. Group-level analysis for the location of S1 revealed a local maximum within the left postcentral gyrus, lying within Brodmann area (BA) 3b as determined by the SPM anatomy toolbox (Eickhoff et al., 2005). In a similar way, V1 was identified by a local maximum within the left calcarine sulcus which was identified as falling within BA 17. The coordinates of the IOG were determined by a local maximum within the left

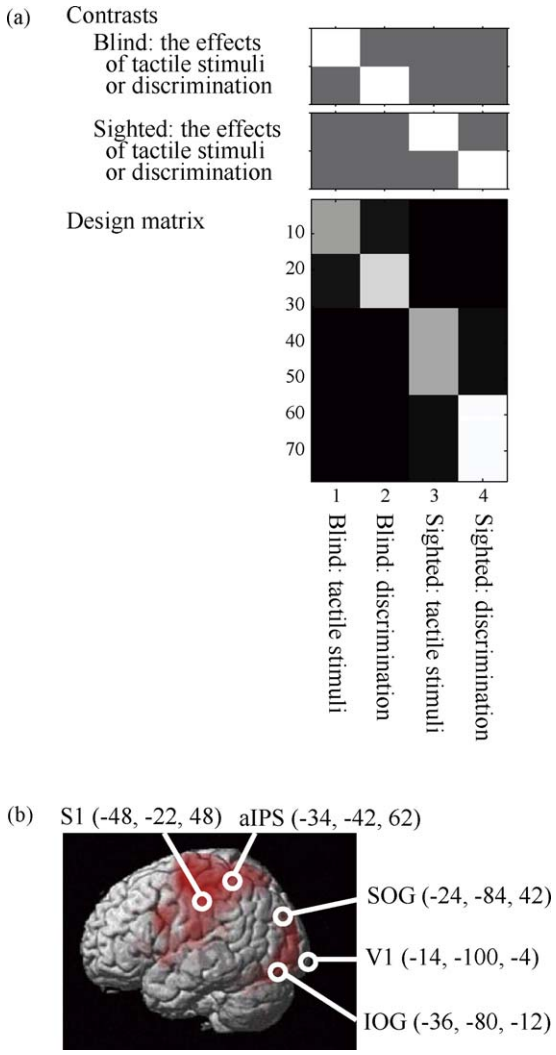

Fig. 1. (a) Design matrix and contrasts of the conjunction analysis. Upper squares represent the *F*-contrasts for the effects of either tactile stimuli or the discrimination task in both blind and sighted groups. The lower square represents the design matrix for the random effects analysis. Each column corresponds to the effect of tactile stimuli or the discrimination task in the bind and sighted groups. (b) Result of the conjunction analysis of the effect of any condition-specific deviation from the overall means in the blind and sighted groups. The regions deactivated in both groups were masked out. White circles indicate the ROIs used by the models. The coordinates shown on the map are the group coordinates.

inferior occipital gyrus, part of the ventral visual stream. The SOG was identified by a local maximum within the left superior occipital gyrus, part of the dorsal visual stream. The aIPS was determined as a local maximum within the anterior intraparietal sulcus. After these group coordinates were defined, the nearest local maximum for each subject was determined for each of the group-level coordinates. Each of these subject-specific local maxima was required to be not further away from each group coordinate than twice the FWHM of the smoothing kernel and to survive a threshold of $p < 0.05$, whole-brain corrected FDR (Genovese et al., 2002). If an individual coordinate was not found, the group coordinate was used as the individual coordinate for that subject. Averaged coordinates of each region in each group and the number of subjects for whom individual coordinates were determined are shown in Table 1. Subject-specific time series were summarized with the principal eigenvariate over voxels within a radius of 4 mm around the individually determined coordinates using the volume-of-interest tool in SPM5.

Coordinates of the IOG in this study corresponded to V4 (Bartels and Zeki, 2000), a region in the ventral stream involved in the processing of visual shape and color information (Grill-Spector and Malach, 2004). The coordinates for the SOG, located at a posterior bank of a transverse occipital sulcus, corresponded to area V3A in the dorsal stream (Tootell et al., 1998). V3A spans the transverse occipital sulcus and extends inferiorly over the lateral portion of the occipital cortex, and has been shown to be sensitive to two-dimensional shape, motion and stereo in humans (Orban et al., 2004; Tootell et al., 1997).

Table 1
Averaged MNI coordinates of each region included in the models.

ROI	Group	*X* mean ± SD	*Y* mean ± SD	*Z* mean ± SD	Found	Missing	Beta for tactile stimuli Mean (%)	Beta for discrimination Mean (%)
S1	Early-blind	−50.7 ± 3.7	−22.2 ± 4.3	48.7 ± 4.7	9	0	1.23	0.23
	Late-blind	−50.3 ± 4.3	−24.0 ± 4.2	50.7 ± 4.7	6	0	2.29	0.09
	Sighted	−50.5 ± 4.9	−22.9 ± 6.5	48.1 ± 6.1	23	1	1.61	0.20
aIPS	Early-blind	−34.0 ± 5.1	−42.7 ± 3.7	65.1 ± 5.8	8	1	1.21	0.45
	Late-blind	−36.7 ± 4.1	−44.7 ± 3.5	62.7 ± 7.0	6	0	1.99	0.01
	Sighted	−37.3 ± 4.2	−42.6 ± 5.3	64.3 ± 4.7	23	1	1.77	0.31
IOG	Early-blind	−33.8 ± 5.5	−79.3 ± 5.7	−11.1 ± 7.6	7	2	0.27	0.45
	Late-blind	−37.3 ± 3.9	−83.0 ± 7.7	−11.7 ± 3.4	6	0	0.53	0.50
	Sighted	−37.2 ± 5.1	−82.0 ± 4.5	−11.3 ± 3.5	19	5	−0.10	−0.27
SOG	Early-blind	−23.8 ± 6.4	−86.4 ± 4.1	40.2 ± 6.9	7	2	0.62	0.38
	Late-blind	−21.7 ± 5.7	−86.7 ± 6.3	42.3 ± 3.4	5	1	0.15	−0.50
	Sighted	−25.3 ± 4.9	−84.3 ± 6.1	43.0 ± 6.0	23	1	−0.27	−0.30
V1	Early-blind	−11.1 ± 4.6	−100.7 ± 5.7	−3.1 ± 5.7	9	0	0.04	0.54
	Late-blind	−10.3 ± 4.5	−103.0 ± 5.5	−4.3 ± 5.3	5	1	0.45	−0.17
	Sighted	−16.0 ± 6.0	−101.1 ± 4.7	−2.8 ± 3.9	21	3	−0.38	−0.26

Abbreviations: S1, primary somatosensory area; aIPS, anterior intraparietal sulcus; IOG, inferior occipital gyrus; SOG, superior occipital gyrus; V1, primary visual area. The "found" column shows the number of subjects for whom individual coordinates fell within the area located twice the FWHM from the group coordinates, while the "missing" column shows the number of subjects for whom individual coordinates were not determined. When no individual coordinate was found, the group coordinate was used as the individual coordinate for that subject. The "beta for tactile stimuli" column shows the beta estimates for the tactile stimuli condition within the ROIs which were averaged in each group. The "beta for discrimination" column shows the values for the discrimination condition.

2.6. Dynamic causal modeling

DCM is based on a bilinear model of neural population dynamics that is combined with a hemodynamic forward model describing the transformation of neural activity into a measured BOLD response (Friston et al., 2003). In DCM, three sets of parameters are estimated: the direct input to a region (i.e., the direct influence of stimuli on regional activity), the baseline connectivity between regions (i.e., the interregional influences in the absence of modulating the experimental context), and the modulation of connectivity between regions (i.e., the changes in the connectivity between regions induced by the experimental context).

2.7. Definition of the models and model selection

We tested two candidate models of cortico-cortical connectivity: (a) a model without direct connectivity between S1 and V1, and (b) a model with direct connectivity between S1 and V1 (Fig. 2). A subcortical pathway candidate was not included, for reasons described in the introduction. As shown in Fig. 2, both models comprised simple bidirectional baseline connectivity across the five regions of interest, with the tactile stimuli driving input into S1. All connections were modulated by the discrimination effect. In addition, the second candidate model (b) had a direct pathway between S1 and V1. We evaluated the baseline connectivity, represented by the connectivity strengths during NDT, and modulation of connectivity, represented by the differences in connectivity during DT and NDT. A generative model of slice timing was used instead of a slice-timing correction when preprocessing the data because of the relatively long repetition time (TR) (Kiebel et al., 2007).

In this study, we defined the neural pathways leading from aIPS–SOG and SOG–V1 as the dorsal visual stream, pathways between IOG and V1 as the ventral visual stream, and connections between aIPS–IOG and SOG–IOG as putative interstream connections between the dorsal and ventral visual streams (Schoenfeld et al., 2003). In fact, the regions which comprise the dorsal stream, such as intraparietal sulcus, MT, and V3A, have connections with regions in the ventral stream such as V4, TEO and TE in non-human primates (Felleman and Van Essen, 1991; Ungerleider et al., 2008; Webster et al., 1994).

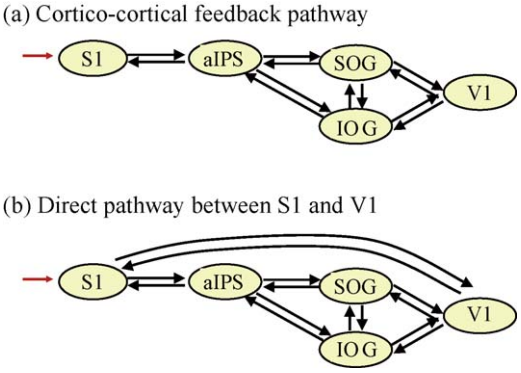

Fig. 2. The two models tested using DCM. Thick black arrows represent connections that are modulated by the discrimination task. Thick red arrows represent direct input by tactile stimuli.

In this study, we used Bayesian model selection (BMS) (Penny et al., 2004) to decide which model was optimal. BMS takes into account not only the relative fit of contrasting models but also their relative complexity. Model evidence, the probability of the data given a particular model, was approximated based on the Akaike information criterion (AIC) and the Bayesian information criterion (BIC). The Bayes factor (BF) is the ratio of the model evidence of two models. Model selection was based on a more conservative BF, which was computed based on AIC or BIC (Penny et al., 2004). A BF of at least e (the natural exponent, 2.7183) was regarded as consistent evidence in favor of one model over another. Following the selection of the optimal model for each blind subject, the optimal model for the entire blind group was determined by the averaged BF (ABF), which is the geometric mean of the Bayes factors for each individual subject. Because the ABF is susceptible to outliers, we also computed the positive evidence ratio (PER), i.e., the number of subjects with positive evidence for the original model divided by the number of subjects with positive evidence for an alternative model (Stephan et al., 2007b).

2.8. Second-level analysis of connectivity parameters

Once the optimal model was identified, differences in directional baseline connectivity and modulation of connectivity across the groups were analyzed. Values of baseline connectivity and the degree of modulation of connectivity were extracted for each subject. First, to show the connectivity patterns within each group, a one-sample *t*-test for early-blind, late-blind and sighted groups were conducted, controlling for FDR within each group (early-blind, late-blind and sighted) and within each type of connectivity parameter (baseline and modulation). Nonparametric testing (Kolmogorov–Smirnoff test) demonstrated that the distribution of connectivity observed in the late-blind group, which is of small sample size, was not different from a normal distribution for each type of connectivity (baseline and modulation), each directed connection (e.g., S1–aIPS) and each group (early-blind, late-blind and sighted). Then, to reveal differences in connectivity parameters between the blind and sighted groups, parameters were entered into a classical second-level (between-subject) independent-samples *t*-test. The test was performed separately for each parameter of each directional connection (e.g., S1–aIPS) and each type of connectivity (baseline vs. modulation). Second, differences in connectivity parameters between early-blind and late-blind groups were also tested with an independent-samples *t*-test for each of the directional connections (e.g., S1–aIPS) and type of connectivity (baseline vs. modulation), controlling for FDR in the same way. To substantiate that the connectivity was dependent on the age of onset of blindness, we performed correlation analyses with the age of onset of blindness. Finally, correlations between accuracy in the discrimination task and the connectivity parameters (baseline connectivity or modulation) of directional connections were computed in the connections which showed differences between the early- and late-blind groups. The statistical threshold was set at $p < 0.05$, corrected for multiple

comparisons using the FDR controlled within each type of connectivity parameter (Benjamini and Hochberg, 1995; Stephan et al., 2007a).

3. Results

3.1. Behavioral results

Accuracy in the discrimination task (percent of correct responses) showed a significant main effect of group ($F_{(2,36)} = 14.5$; $p < 0.001$, one-way ANOVA). Also, post hoc tests revealed that the accuracy of the early-onset blind group ($80.7 \pm 12.4\%$) was significantly higher than that of the late-onset blind ($57.8 \pm 14.9\%$; $p < 0.001$) and sighted ($65.6 \pm 10.0\%$; $p < 0.001$) groups.

3.2. Bayesian model selection in the blind group

We compared the two models across all the blind subjects by Bayesian model selection using the ABF and PER values as indices. The optimal model was found to be model (a), which lacks direct connectivity between S1 and V1 (Fig. 2). Comparison of model (a) with model (b) showed that the ABF was 82.9 and the PER was 12:0. These indicate that the balance between data fit and model complexity of model (a) is on average 82.9 times higher than that of model (b), and that positive evidence for model (a) was observed in 12 out of 15 subjects, whereas no subject showed positive evidence for model (b). These results suggest that model (a), lacking direct connectivity between S1 and V1, was more successful than the alternative model at describing the functional imaging data from the blind group.

Similar results were found when the blind group was divided into sub-groups of early- and late-blind participants. In the early-blind group, comparison of model (a) with model (b) produced an ABF of 9.4 and PER of 6:0. In the late-blind group, comparing model (a) with model (b) yielded an ABF of 2160.4 and PER of 6:0. Thus, BMS showed that, for both early- and late-blind groups, model (a) was optimal. The optimal model (a) for the blind group was then applied to the sighted group for further analysis.

3.3. Second-level analysis of connectivity parameters

A summary of the group results of the one-sample *t*-tests is shown in Fig. 3, in which only significant connectivity is shown. These *t*-tests simply test the null hypothesis that connection is zero, against the between subject variability in coupling strength. Baseline connectivity and modulation of connectivity showed a similar pattern across all groups. For the early-onset blind group, the dorsal pathway showed robust connectivity from aIPS through SOG to V1. The IOG showed significant reciprocal connectivity with SOG and unidirectional connectivity from aIPS. In the late-onset blind group, there were fewer significant connections than in the other groups, probably because of the smaller sample size. For the sighted group, aIPS showed negative unidirectional connectivity to SOG and bidirectional negative connectivity with IOG, while IOG and V1 shared positive connectivity.

To show the influence of blindness on the connectivity patterns, we compared the connectivity parameters between the blind and sighted groups. There were significant differences in the bidirectional connectivity of both the baseline connectivity and the modulation of connectivity in aIPS–SOG and aIPS–IOG (FDR corrected $p < 0.05$). As shown in Fig. 4, in the blind group the connectivity parameters in aIPS–SOG and aIPS–IOG were positive, while they were negative in the sighted group. Baseline connectivity and modulation of connectivity showed similar patterns in both groups.

Furthermore, to show the effect of the age of onset of blindness on connectivity, we compared the connectivity parameters between the early- and late-blind groups. The early-blind group showed higher connectivity parameters in the dorsal pathway than the late-blind group in both baseline connectivity and the modulation of connectivity (baseline connectivity: aIPS–SOG, SOG–V1, and V1–SOG; modulation of connectivity: aIPS–SOG and SOG–V1; FDR corrected $p < 0.05$) and the interstream connections (baseline connectivity and modulation of connectivity: SOG–IOG and IOG–SOG; FDR corrected $p < 0.05$; Fig. 5).

To confirm the dependency of the connectivity patterns on the age of onset of blindness, we conducted correlation analyses with

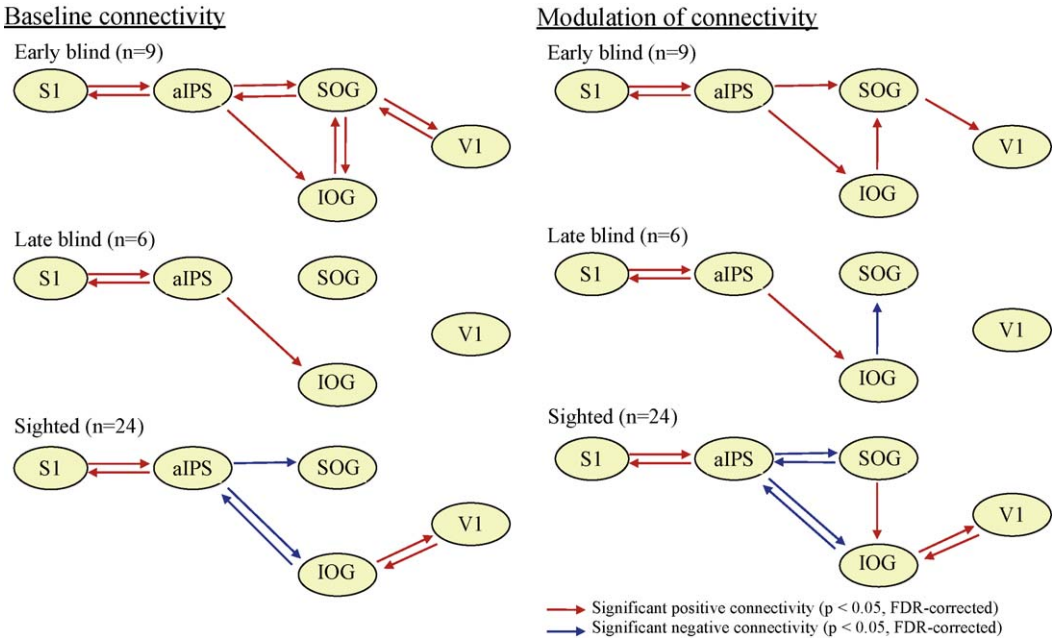

Fig. 3. Summary of one-sample *t*-tests in blind and sighted groups. Only significant baseline connectivity and significant modulation of connectivity are shown. Red arrows indicate positive connectivity parameters and blue arrows depict negative connectivity parameters. Baseline connectivity and modulation of connectivity are shown separately.

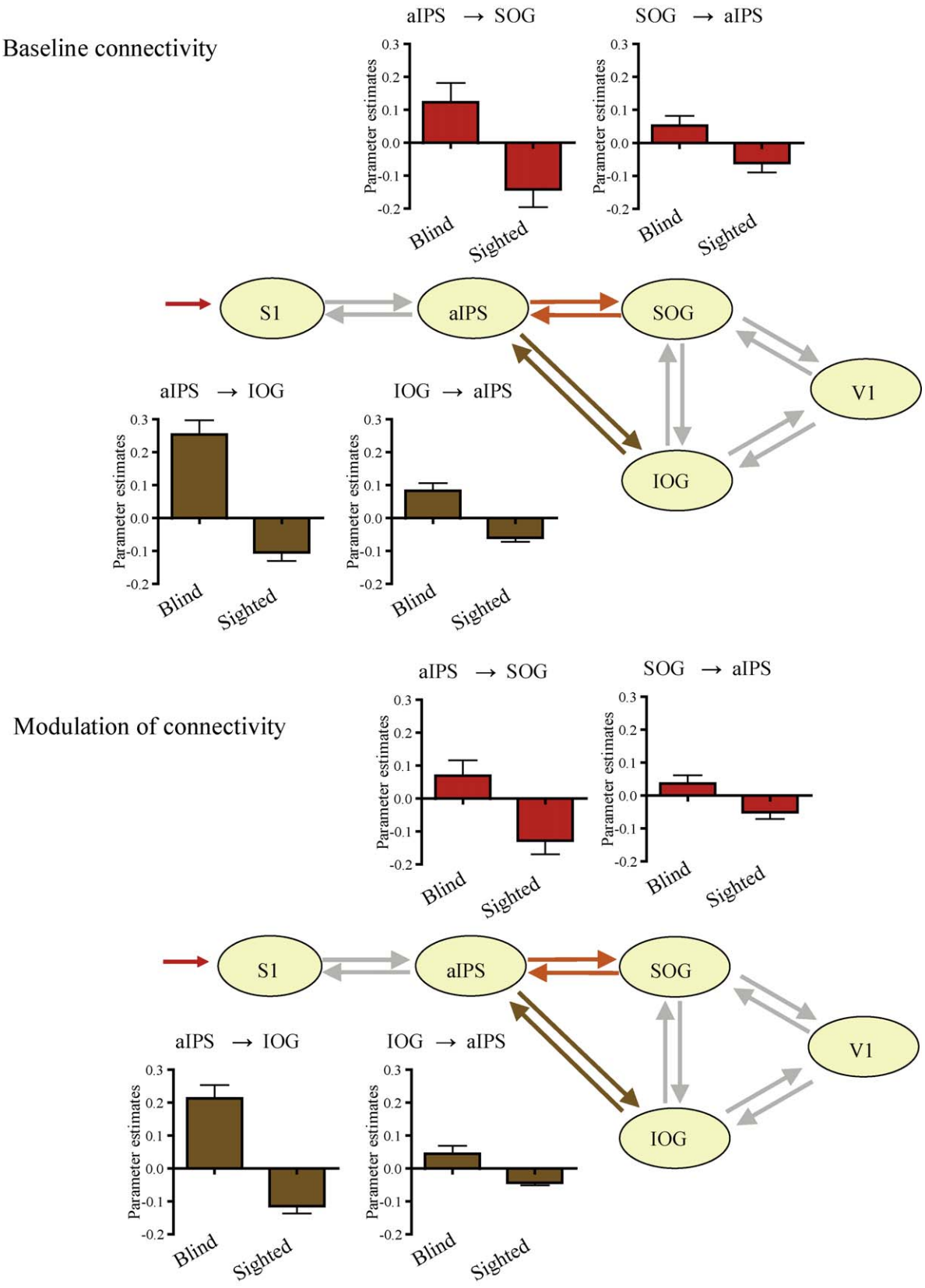

Fig. 4. Comparison of connectivity parameters between the blind and sighted groups. The upper portion of the figure represents the parameters of the baseline connectivity, while the lower part of the figure shows the modulation of connectivity. All of the colored solid connections (aIPS–SOG and aIPS–IOG) showed group differences between the blind and sighted groups (FDR corrected $p < 0.05$). Each graph shows the connectivity parameters of each directed connection. Bars and error bars represent mean and SEM values.

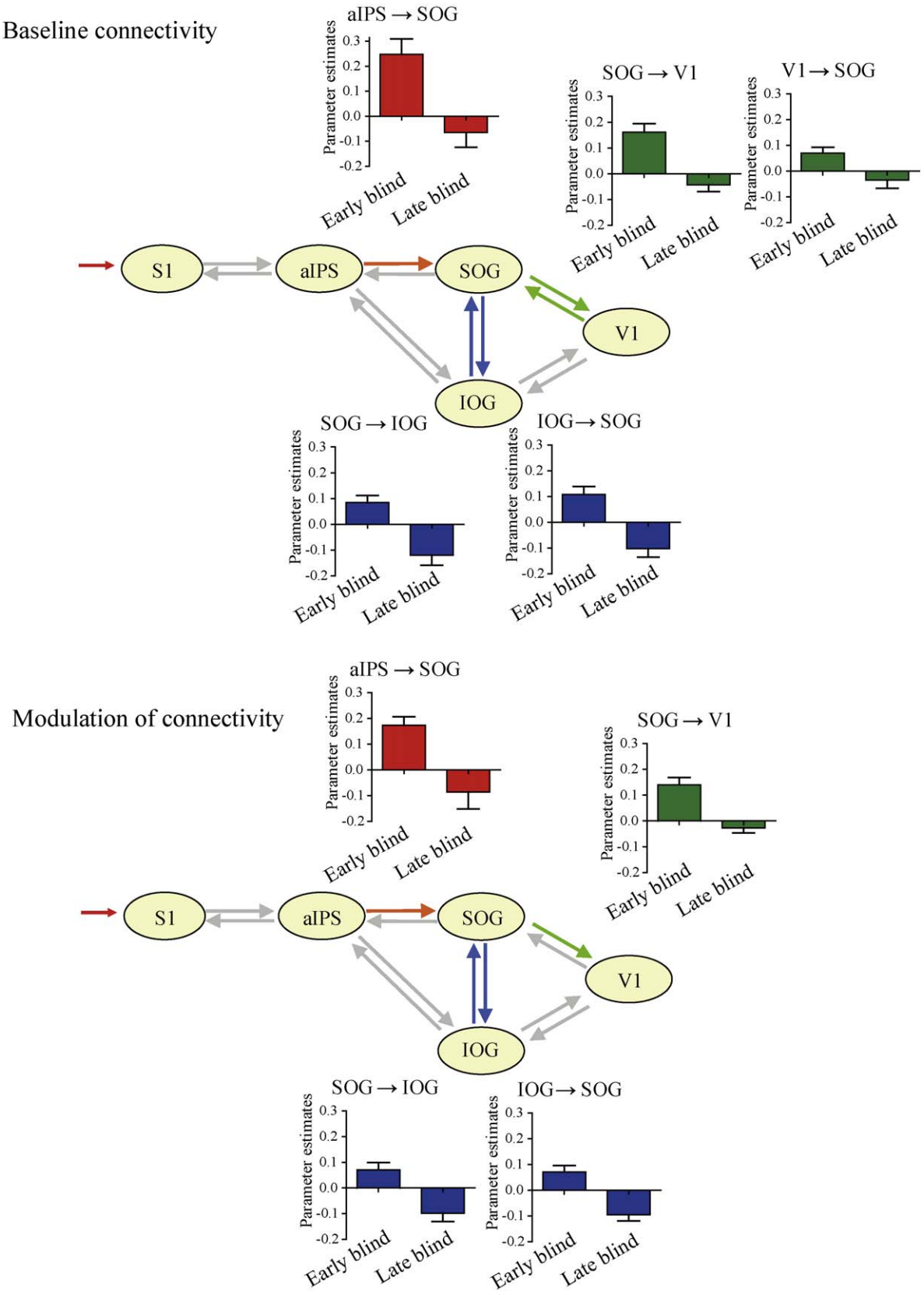

Fig. 5. Comparison of the connectivity parameters between the early- and late-blind groups. The upper part of the figure represents the parameters of baseline connectivity while the lower section of the figure shows the modulation of connectivity. All the colored connections (aIPS–SOG, SOG–V1 and SOG–IOG) showed group differences between early- and late-blind groups (FDR corrected $p < 0.05$). Each graph shows the connectivity parameters of each directed connection. Bars and error bars represent mean and SEM values.

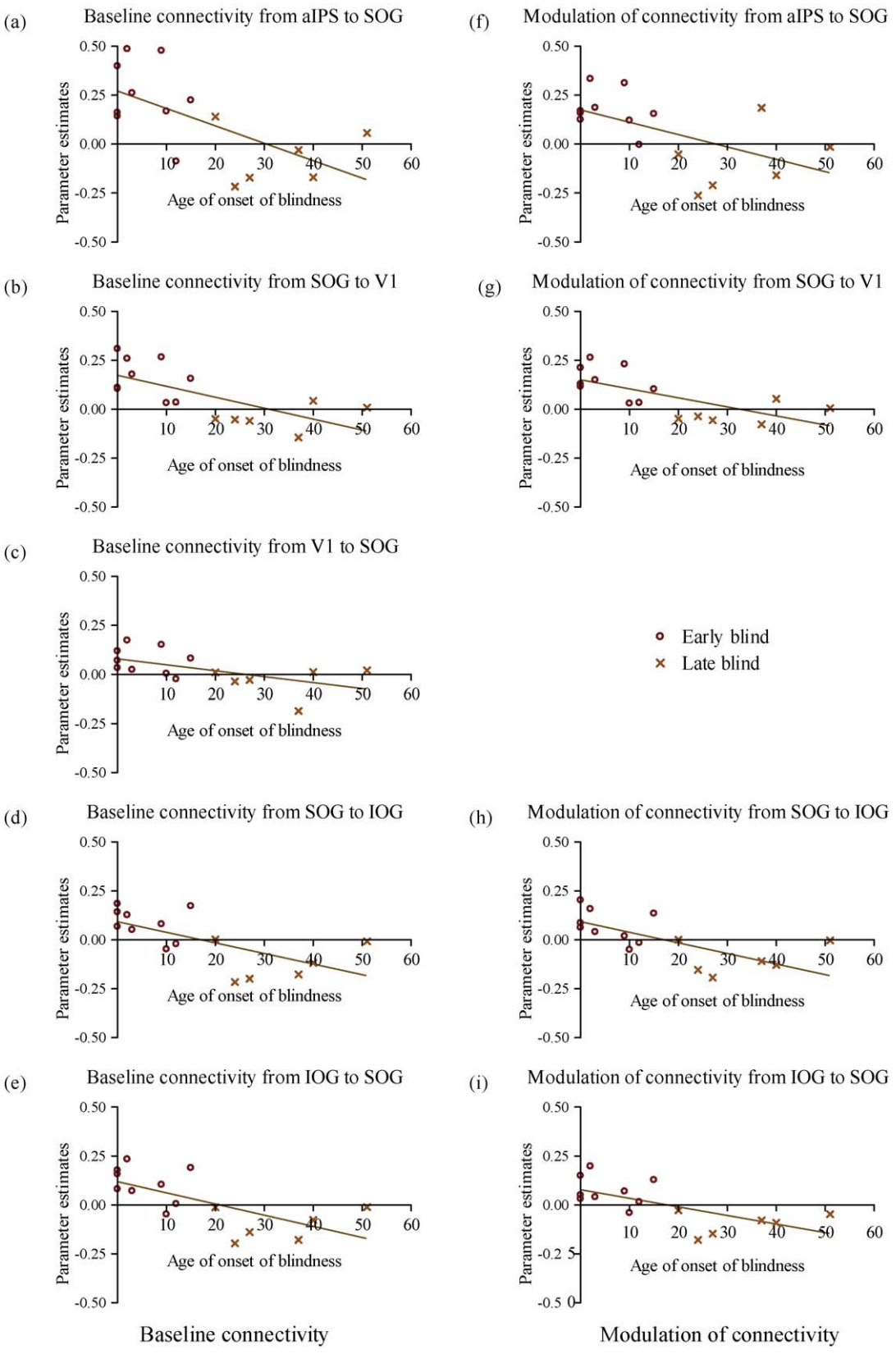

Fig. 6. *Left column*: Parameter estimates of baseline connectivity in the dorsal pathway from aIPS to SOG (a), from SOG to V1 (b), from V1 to SOG (c), and in the interstream connections from SOG to IOG (d) and from IOG to SOG (e) plotted against the age of onset of blindness. Each open circle represents a subject in the early-blind group while each x represents a subject in the late-blind group. There was a significant negative correlation in the dorsal pathway (aIPS–SOG, $r = -0.63$; SOG–V1, $r = -0.67$; V1–SOG, $r = -0.56$; FDR corrected $p < 0.05$) and in the interstream connections (SOG–IOG, $r = -0.66$; IOG–SOG, $r = -0.68$; FDR corrected $p < 0.05$). *Right column*: Parameter estimates of the modulation of connectivity in the dorsal pathway from aIPS to SOG (f) and from SOG to V1 (g), and in the interstream connections from SOG to IOG (h) and from IOG to SOG (i) plotted against the age of onset of blindness. There was a significant negative correlation in the dorsal pathway (aIPS–SOG, $r = -0.57$; SOG–V1, $r = -0.69$; FDR corrected $p < 0.05$) and in the interstream connections (SOG–IOG, $r = -0.65$; IOG–SOG, $r = -0.66$; FDR corrected $p < 0.05$).

the age of onset of blindness. Age of onset of blindness was negatively correlated with baseline connectivity in the dorsal pathway (aIPS–SOG, $r = -0.63$; SOG–V1, $r = -0.67$; V1–SOG, $r = -0.56$; FDR corrected $p < 0.05$; Fig. 6, left column) and the interstream connections (SOG–IOG, $r = -0.66$; IOG–SOG, $r = -0.68$; FDR corrected $p < 0.05$; Fig. 6, left column). Age of onset of blindness also correlated with the modulation of connectivity in the dorsal pathway (aIPS–SOG, $r = -0.57$; SOG–V1, $r = -0.69$; FDR corrected $p < 0.05$; Fig. 6, right column) and the interstream connections (SOG–IOG, $r = -0.65$; IOG–SOG, $r = -0.66$; FDR corrected $p < 0.05$; Fig. 6, right column).

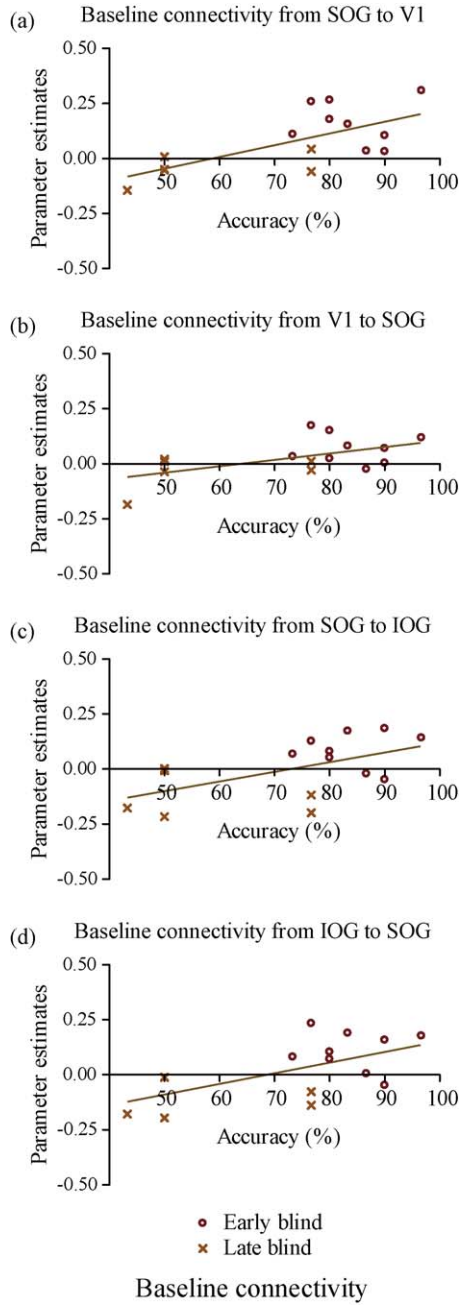

Fig. 7. Parameter estimates of the baseline connectivity in the dorsal pathway from SOG to V1 (a) and from V1 to SOG (b), and the interstream connections from SOG to IOG (c) and from IOG to SOG (d) plotted against accuracy on the Braille discrimination task. Each open circle represents one subject in the early-blind group while each x represents a subject in the late-blind group. There was a significant positive correlation in the dorsal pathway (SOG–V1, $r = 0.68$; V1–SOG, $r = 0.57$; FDR corrected $p < 0.05$) and in the interstream connections (SOG–IOG, $r = 0.56$; IOG–SOG, $r = 0.61$; FDR corrected $p < 0.05$).

3.4. Correlation with performance

In the blind group, accuracy in the discrimination task was positively correlated with baseline connectivity in the dorsal pathway (SOG–V1, $r = 0.68$; V1–SOG, $r = 0.57$; FDR corrected $p < 0.05$; Fig. 7) and the interstream connections (SOG–IOG, $r = 0.56$; IOG–SOG, $r = 0.61$; FDR corrected $p < 0.05$; Fig. 7). These results showed that higher connectivity in the interstream connections and the dorsal pathway was related to better tactile discrimination performance in blind subjects.

4. Discussion

4.1. Input to the striate cortex through a cortico-cortical feedback pathway

We have investigated the input pathway to the striate cortex by means of fMRI and DCM. Bayesian model selection showed that modeling of a cortico-cortical feedback pathway without direct connectivity between S1 and V1 was optimal at describing the imaging data of early- and late-blind groups collected during tactile Braille tasks. The additive assumption of bidirectional connections between S1 and V1 in model (b) did not improve the fit of the data to an extent that would compensate for the increased complexity of the model, suggesting that connectivity changes due to visual deprivation may result from modifications of the connections which already exist in sighted people.

The V1 ROI (averaged MNI coordinates −14, −100, −4) is located at the occipital pole, and may therefore correspond to the central visual field in sighted individuals. A non-human primate study showed that the connectivity of area 17 (primary visual cortex) is eccentricity dependent: peripheral area 17 receives projections from the auditory cortex and polysensory STP, whereas central area 17 does not (Falchier et al., 2002). Faichler et al. observed no direct projection from S1 to V1. They speculated that the tactile–visual cross-modal reorganization is related to the projection from S1 through the polymodal STP to peripheral area 17. This is consistent with the preferential recruitment of peripheral V1 during Braille reading in blind people (Burton et al., 2002; Burton, 2003; Bucher et al., 2006).

In our model, the connectivity between central V1 and S1 through peripheral V1 is represented by direct connectivity, as we did not include an ROI in the peripheral V1. Bayesian model comparison showed that the model without direct connection between S1 and V1 was superior to that with direct connectivity. Thus we concluded that direct connectivity (even through peripheral V1) is unlikely to occur in the early blind.

4.2. Robustness of connectivity evaluation

There were challenges in the selection of common ROIs and in the between-group model fitting analyses. For the ROI analyses, we selected regions which were perturbed positively or negatively in both blind and sighted groups, and which reached significance in the *F*-test and conjunction analyses. The five regions selected may not, therefore, be appropriate for the blind and sighted groups individually. Furthermore, the amount of influence between one region and another (represented by the connectivity parameters) might include both direct and indirect influences. We separately analyzed the data using group coordinates, which replicated the results based on the individually determined ROIs (Supplementary Figures S1 and S2). Model (a) was preferred to model (b) with an ABF of 13.93 and PER of 11:0. The blind group showed higher

baseline connectivity and modulation of connectivity than the sighted group in intermodal connectivity (aIPS–SOG and aIPS–IOG) (for details, see Supplementary Figure S1). Furthermore, the early-blind group showed higher connectivity and modulation of connectivity than the late-blind group in the dorsal pathway (aIPS–SOG and SOG–V1) and in the interstream connection between SOG and IOG (for details, see Supplementary Figure S2). Thus, the present findings are robust to possible anatomical variation across subjects, and sufficient to test our hypothesis. However, this does not necessarily exclude the contribution of other pathways, as neurological changes following sensory deprivation are likely to vary greatly, and depend on multiple mechanisms, depending on the nature and timing of the altered experiences (Bavelier and Neville, 2002).

4.3. Modality border

The present study found negative connectivity from aIPS to SOG and IOG in the sighted group. The negative values of baseline connectivity and modulation of connectivity between tactile and visual processing areas in the sighted group can be interpreted as an inhibitory inter-modal processing effect, as increases in activity in tactile processing regions has been associated with decreased activity in visual processing areas (Plailly et al., 2008). Thus, the negative connectivity may represent the border of the functional segregation between the tactile and visual modalities in the sighted subjects. In fact, we showed that in the sighted group only S1 and aIPS shared positive connectivity, and these regions were negatively connected with SOG and IOG. In contrast, in the blind group, tactile and visual processing areas were positively connected. This is consistent with the notion that visual deprivation modifies the interregional effective connectivity, such that a competitive imbalance between tactile and visual inputs causes a shift of the neural modality border (Rauschecker, 1995) in an age-independent manner. The modality border refers to the boundary between regions processing one kind of sensory input and another. In the context of effective connectivity, this is expressed as negative connectivity. Changes of functional segregation by cortical plasticity can be demonstrated with a shift of modality border.

The LOC, one of the regions in the ventral visual stream, is known to be activated by both visual and tactile object recognition (Amedi et al., 2001). A relatively rapid expansion of the tactile modalities into the visual areas, including the lateral occipital region (LO) and V1, was shown in experiments where sighted participants were blindfolded for 5 days (Merabet et al., 2008; Pascual-Leone et al., 2005; Pascual-Leone and Hamilton, 2001). These findings suggest that bimodal areas in the ventral visual pathways may be a primary location for tactile–visual effective competition.

4.4. Age dependency of onset of blindness and task specificity

In the early-onset blind group, regions of the dorsal visual stream leading to the striate cortex showed significant positive connectivity (Fig. 3), indicating that the dorsal stream may be the main input pathway to the striate cortex. Main effects of the age of onset of blindness were confined to the dorsal stream and one interstream connection, SOG–IOG (Figs. 5 and 6). The effective connectivity of the dorsal pathway and the SOG–IOG interstream connection showed a positive correlation with performance on the Braille tactile discrimination task across blind subjects. This is consistent with previous studies showing the functional relevance of the striate cortex in early-blind individuals (Cohen et al., 1999; Sadato et al., 2002).

Increased effective connectivity of the dorsal pathway to the striate cortex in early-blind subjects might be related to the nature of form discrimination within the modality of touch, which has been described as dynamic perception (Nakada and Dellon, 1989). In the present study, we used a passive tactile discrimination task in which subjects were presented with tactile stimuli to the fingertip without the opportunity to engage in active tactile exploration. The tactile stimuli consisted of coherently moving dots forming a Braille character. Subjects were required to recognize what kind of shape the coherently moving dots formed. This process is very similar to the form-from-motion task, which is used mainly in the visual modality (Bucher et al., 2006; Schoenfeld et al., 2003; Schrauf et al., 1999). Form-from-motion stimuli are a subset of visual stimuli consisting of dots which move coherently to create the appearance of a simple form. Using magnetoencephalography (MEG), Schoenfeld et al. (2003) showed that in sighted people, after early activation of low-level visual cortical areas, visual form-from-motion stimuli are processed sequentially: first, the stimuli are analyzed in the dorsal visual region, MT/V5, which extracts motion information, and then relays information to the ventral visual region, LO, and inferior temporal (IT) cortex, for form analysis. In contrast, form-from-luminance stimuli are processed only in LO and IT without MT/V5 involvement (Schoenfeld et al., 2003). These findings are supported by fMRI data (Bucher et al., 2006), which demonstrate that performance in visual form-from-motion tasks in sighted children reaches the level of adult proficiency at the age of 15 years, while proficiency in luminance-based visual acuity and form perception matures by age 7 years (Bucher et al., 2006; Schrauf et al., 1999). Schrauf et al. (1999) suggested that visual form detection based on motion contrast is processed separately from that based on luminance contrast. Furthermore, integration of visual and haptic form information is unstable at 8–10 years of age (Gori et al., 2008). Gori et al. suggested that delayed integration of visuo-haptic cross-sensory form information is caused by continuous recalibration during development to take physical growth into account.

These findings indicate that the neural substrates of visual form-from-motion processing may be less confined to the visual modality through adolescence. This raises the possibility that some neural centers for dynamic form-from-motion processing in the dorsal visual pathway, probably including striate cortex, may accept tactile information in order to process tactile form-from-motion when visual input is deprived. Thus, the acquisition of Braille-reading skills after early development (up to adolescence) may profit by the recruitment of the visual cortical resources that have been deprived of visual input.

4.5. Conclusion

We used fMRI and DCM to investigate the input pathways to striate cortex during a Braille discrimination task in early-onset blind participants. Our results suggest that cortico-cortical feedback from multimodal areas through the dorsal visual stream may be a main input pathway to V1 in early-blind subjects, and early visual deprivation may induce the plastic enhancement of the dorsal stream for tactile processing, resulting in better performance in Braille reading. In contrast, irrespective of the age of onset of blindness, tactile processing areas may expand into the ventral visual regions, due to the competitive imbalance caused by the loss of visual input.

Authors' contributions

- TF carried out the data analysis and drafted the manuscript.
- HCT participated in the data analysis and revision of the manuscript.
- TK participated in the data analysis.

- NS participated in the task and study design, data analysis and revision of the manuscript.
- All authors read and approved the final manuscript.

Acknowledgments

This study was supported in part by Grant-in Aid for Scientific Research S#17100003 and S#21220005 (both to NS) from the Japan Society for the Promotion of Science.

Appendix A. Supplementary data

Supplementary data associated with this article can be found, in the online version, at doi:10.1016/j.neures.2009.06.014.

References

Amedi, A., Malach, R., Hendler, T., Peled, S., Zohary, E., 2001. Visuo-haptic object-related activation in the ventral visual pathway. Nat. Neurosci. 4, 324–330.
Amedi, A., Raz, N., Pianka, P., Malach, R., Zohary, E., 2003. Early 'visual' cortex activation correlates with superior verbal memory performance in the blind. Nat. Neurosci. 6, 758–766.
Amedi, A., Stern, W.M., Camprodon, J.A., Bermpohl, F., Merabet, L., Rotman, S., et al., 2007. Shape conveyed by visual-to-auditory sensory substitution activates the lateral occipital complex. Nat. Neurosci. 10, 687–689.
Bartels, A., Zeki, S., 2000. The architecture of the colour centre in the human visual brain: new results and a review. Eur. J. Neurosci. 12, 172–193.
Bavelier, D., Neville, H.J., 2002. Cross-modal plasticity: where and how? Nat. Rev. Neurosci. 3, 443–452.
Benjamini, Y., Hochberg, Y., 1995. Controlling the false discovery rate—a practical and powerful approach to multiple testing. J. Roy. Stat. Soc. Ser. B: Methodol. 57, 289–300.
Bitan, T., Booth, J.R., Choy, J., Burman, D.D., Gitelman, D.R., Mesulam, M.M., 2005. Shifts of effective connectivity within a language network during rhyming and spelling. J. Neurosci. 25, 5397–5403.
Bremmer, F., Schlack, A., Shah, N.J., Zafiris, O., Kubischik, M., Hoffmann, K., et al., 2001. Polymodal motion processing in posterior parietal and premotor cortex: a human fMRI study strongly implies equivalencies between humans and monkeys. Neuron 29, 287–296.
Bronchti, G., Heil, P., Scheich, H., Wollberg, Z., 1989. Auditory pathway and auditory activation of primary visual targets in the blind mole rat (*Spalax ehrenbergi*). I. 2-Deoxyglucose study of subcortical centers. J. Comp. Neurol. 284, 253–274.
Bucher, K., Dietrich, T., Marcar, V.L., Brem, S., Halder, P., Boujraf, S., et al., 2006. Maturation of luminance- and motion-defined form perception beyond adolescence: a combined ERP and fMRI study. Neuroimage 31, 1625–1636.
Burton, H., Snyder, A.Z., Conturo, T.E., Akbudak, E., Ollinger, J.M., Raichle, M.E., 2002. Adaptive changes in early and late blind: a fMRI study of Braille reading. J. Neurophysiol. 87, 589–607.
Burton, H., 2003. Visual cortex activity in early and late blind people. J. Neurosci. 23, 4005–4011.
Cohen, L.G., Celnik, P., Pascual-Leone, A., Corwell, B., Falz, L., Dambrosia, J., et al., 1997. Functional relevance of cross-modal plasticity in blind humans. Nature 389, 180–183.
Cohen, L.G., Weeks, R.A., Sadato, N., Celnik, P., Ishii, K., Hallett, M., 1999. Period of susceptibility for cross-modal plasticity in the blind. Ann. Neurol. 45, 451–460.
Driver, J., Noesselt, T., 2008. Multisensory interplay reveals crossmodal influences on 'sensory-specific' brain regions, neural responses, and judgments. Neuron 57, 11–23.
Eickhoff, S.B., Stephan, K.E., Mohlberg, H., Grefkes, C., Fink, G.R., Amunts, K., et al., 2005. A new SPM toolbox for combining probabilistic cytoarchitectonic maps and functional imaging data. Neuroimage 25, 1325–1335.
Falchier, A., Clavagnier, S., Barone, P., Kennedy, H., 2002. Anatomical evidence of multimodal integration in primate striate cortex. J. Neurosci. 22, 5749–5759.
Felleman, D.J., Van Essen, D.C., 1991. Distributed hierarchical processing in the primate cerebral cortex. Cereb. Cortex 1, 1–47.
Friston, K.J., 1994. Functional and effective connectivity in neuroimaging: a synthesis. Hum. Brain Mapp. 2, 56–78.
Friston, K.J., Harrison, L., Penny, W., 2003. Dynamic causal modelling. Neuroimage 19, 1273–1302.
Friston, K.J., Penny, W.D., Glaser, D.E., 2005. Conjunction revisited. Neuroimage 25, 661–667.
Genovese, C.R., Lazar, N.A., Nichols, T., 2002. Thresholding of statistical maps in functional neuroimaging using the false discovery rate. Neuroimage 15, 870–878.
Gori, M., Del Viva, M., Sandini, G., Burr, D.C., 2008. Young children do not integrate visual and haptic form information. Curr. Biol. 18, 694–698.
Grefkes, C., Weiss, P.H., Zilles, K., Fink, G.R., 2002. Crossmodal processing of object features in human anterior intraparietal cortex: an fMRI study implies equivalencies between humans and monkeys. Neuron 35, 173–184.
Grill-Spector, K., Malach, R., 2004. The human visual cortex. Annu. Rev. Neurosci. 27, 649–677.
Grol, M.J., Majdandzic, J., Stephan, K.E., Verhagen, L., Dijkerman, H.C., Bekkering, H., et al., 2007. Parieto-frontal connectivity during visually guided grasping. J. Neurosci. 27, 11877–11887.
Hamilton, R., Keenan, J.P., Catala, M., Pascual-Leone, A., 2000. Alexia for Braille following bilateral occipital stroke in an early blind woman. Neuroreport 11, 237–240.
Harada, T., Saito, D.N., Kashikura, K., Sato, T., Yonekura, Y., Honda, M., et al., 2004. Asymmetrical neural substrates of tactile discrimination in humans: a functional magnetic resonance imaging study. J. Neurosci. 24, 7524–7530.
Holmes, A.P., Friston, K.J., 1998. Generalisability, random effects & population inference. Neuroimage 7, S754.
Kayser, C., Logothetis, N.K., 2007. Do early sensory cortices integrate cross-modal information? Brain Struct. Funct. 212, 121–132.
Kiebel, S.J., Kloppel, S., Weiskopf, N., Friston, K.J., 2007. Dynamic causal modeling: a generative model of slice timing in fMRI. Neuroimage 34, 1487–1496.
Kujala, T., Huotilainen, M., Sinkkonen, J., Ahonen, A.I., Alho, K., Hamalainen, M.S., et al., 1995. Visual cortex activation in blind humans during sound discrimination. Neurosci. Lett. 183, 143–146.
Kumar, S., Stephan, K.E., Warren, J.D., Friston, K.J., Griffiths, T.D., 2007. Hierarchical processing of auditory objects in humans. PLoS Comput. Biol. 3, e100.
Lakatos, P., Chen, C.M., O'Connell, M.N., Mills, A., Schroeder, C.E., 2007. Neuronal oscillations and multisensory interaction in primary auditory cortex. Neuron 53, 279–292.
Leclerc, C., Saint-Amour, D., Lavoie, M.E., Lassonde, M., Lepore, F., 2000. Brain functional reorganization in early blind humans revealed by auditory event-related potentials. Neuroreport 11, 545–550.
Martuzzi, R., Murray, M.M., Michel, C.M., Thiran, J.P., Maeder, P.P., Clarke, S., et al., 2007. Multisensory interactions within human primary cortices revealed by BOLD dynamics. Cereb. Cortex 17, 1672–1679.
Merabet, L.B., Hamilton, R., Schlaug, G., Swisher, J.D., Kiriakopoulos, E.T., Pitskel, N.B., et al., 2008. Rapid and reversible recruitment of early visual cortex for touch. PLoS ONE 3, e3046.
Mishkin, M., Ungerleider, L.G., Macko, K.A., 1983. Object vision and spatial vision. 2. Cortical pathways. Trends Neurosci. 6, 414–417.
Nakada, M., Dellon, A.L., 1989. Relationship between sensibility and ability to read Braille in diabetics. Microsurgery 10, 138–141.
Noppeney, U., Friston, K.J., Ashburner, J., Frackowiak, R., Price, C.J., 2005. Early visual deprivation induces structural plasticity in gray and white matter. Curr. Biol. 15, R488–R490.
Oldfield, R.C., 1971. The assessment and analysis of handedness: the Edinburgh inventory. Neuropsychologia 9, 97–113.
Orban, G.A., Van Essen, D., Vanduffel, W., 2004. Comparative mapping of higher visual areas in monkeys and humans. Trends Cogn. Sci. 8, 315–324.
Pascual-Leone, A., Amedi, A., Fregni, F., Merabet, L.B., 2005. The plastic human brain cortex. Annu. Rev. Neurosci. 28, 377–401.
Pascual-Leone, A., Hamilton, R., 2001. The metamodal organization of the brain. Prog. Brain Res. 134, 427–445.
Penny, W.D., Stephan, K.E., Mechelli, A., Friston, K.J., 2004. Comparing dynamic causal models. Neuroimage 22, 1157–1172.
Plailly, J., Howard, J.D., Gitelman, D.R., Gottfried, J.A., 2008. Attention to odor modulates thalamocortical connectivity in the human brain. J. Neurosci. 28, 5257–5267.
Ptito, M., Moesgaard, S.M., Gjedde, A., Kupers, R., 2005. Cross-modal plasticity revealed by electrotactile stimulation of the tongue in the congenitally blind. Brain 128, 606–614.
Rauschecker, J.P., 1995. Compensatory plasticity and sensory substitution in the cerebral cortex. Trends Neurosci. 18, 36–43.
Rockland, K.S., Ojima, H., 2003. Multisensory convergence in calcarine visual areas in macaque monkey. Int. J. Psychophysiol. 50, 19–26.
Roder, B., Teder-Salejarvi, W., Sterr, A., Rosler, F., Hillyard, S.A., Neville, H.J., 1999. Improved auditory spatial tuning in blind humans. Nature 400, 162–166.
Sadato, N., Okada, T., Honda, M., Yonekura, Y., 2002. Critical period for cross-modal plasticity in blind humans: a functional MRI study. Neuroimage 16, 389–400.
Sadato, N., Pascual-Leone, A., Grafman, J., Ibanez, V., Deiber, M.P., Dold, G., et al., 1996. Activation of the primary visual cortex by Braille reading in blind subjects. Nature 380, 526–528.
Sadato, N., Pascual-Leone, A., Grafman, J., Deiber, M.P., Ibanez, V., Hallett, M., 1998. Neural networks for Braille reading by the blind. Brain 121 (Pt 7), 1213–1229.
Sadato, N., Okada, T., Kubota, K., Yonekura, Y., 2004. Tactile discrimination activates the visual cortex of the recently blind naive to Braille: a functional magnetic resonance imaging study in humans. Neurosci. Lett. 359, 49–52.
Schoenfeld, M.A., Woldorff, M., Duzel, E., Scheich, H., Heinze, H.J., Mangun, G.R., 2003. Form-from-motion: MEG evidence for time course and processing sequence. J. Cogn. Neurosci. 15, 157–172.
Schrauf, M., Wist, E.R., Ehrenstein, W.H., 1999. Development of dynamic vision based on motion contrast. Exp. Brain Res. 124, 469–473.
Shimony, J.S., Burton, H., Epstein, A.A., McLaren, D.G., Sun, S.W., Snyder, A.Z., 2006. Diffusion tensor imaging reveals white matter reorganization in early blind humans. Cereb. Cortex 16, 1653–1661.
Stephan, K.E., Marshall, J.C., Penny, W.D., Friston, K.J., Fink, G.R., 2007a. Interhemispheric integration of visual processing during task-driven lateralization. J. Neurosci. 27, 3512–3522.

Stephan, K.E., Weiskopf, N., Drysdale, P.M., Robinson, P.A., Friston, K.J., 2007b. Comparing hemodynamic models with DCM. Neuroimage 38, 387–401.
Tootell, R.B., Mendola, J.D., Hadjikhani, N.K., Ledden, P.J., Liu, A.K., Reppas, J.B., et al., 1997. Functional analysis of V3A and related areas in human visual cortex. J. Neurosci. 17, 7060–7078.
Tootell, R.B.H., Hadjikhani, N.K., Mendola, J.D., Marrett, S., Dale, A.M., 1998. From retinotopy to recognition: fMRI in human visual cortex. Trend Cogn. Sci. 2, 174–183.
Uhl, F., Franzen, P., Lindinger, G., Lang, W., Deecke, L., 1991. On the functionality of the visually deprived occipital cortex in early blind persons. Neurosci. Lett. 124, 256–259.
Ungerleider, L.G., Galkin, T.W., Desimone, R., Gattass, R., 2008. Cortical connections of area V4 in the macaque. Cereb. Cortex 18, 477–499.
Wanet-Defalque, M.C., Veraart, C., De Volder, A., Metz, R., Michel, C., Dooms, G., et al., 1988. High metabolic activity in the visual cortex of early blind human subjects. Brain Res. 446, 369–373.
Webster, M.J., Bachevalier, J., Ungerleider, L.G., 1994. Connections of inferior temporal areas TEO and TE with parietal and frontal cortex in macaque monkeys. Cereb. Cortex 4, 470–483.
Weeks, R., Horwitz, B., Aziz-Sultan, A., Tian, B., Wessinger, C.M., Cohen, L.G., et al., 2000. A positron emission tomographic study of auditory localization in the congenitally blind. J. Neurosci. 20, 2664–2672.
Wittenberg, G.F., Werhahn, K.J., Wassermann, E.M., Herscovitch, P., Cohen, L.G., 2004. Functional connectivity between somatosensory and visual cortex in early blind humans. Eur. J. Neurosci. 20, 1923–1927.